Pharm Res (2014) 31:2857–2867
DOI 10.1007/s11095-014-1382-7

RESEARCH PAPER

Azithromycin Cationic Non-Lecithoid Nano/Microparticles Improve Bioavailability and Targeting Efficiency

Meng Zhong • Yue Feng • Hong Liao • Xueyuan Hu • Shengli Wan • Biyue Zhu • Mi Zhang • Huarong Xiong • Yunli Zhou • Jingqing Zhang

Received: 23 December 2013 / Accepted: 7 April 2014 / Published online: 11 September 2014

ABSTRACT

Purpose The purpose of this study was to develop and evaluate the azithromycin cationic non-lecithoid nano/microparticles with high bioavailability and lung targeting efficiency.

Methods The cationic niosomes with different sizes (AMCNS-S and AMCNS-L) along with varied built-in characteristics were produced to achieve high bioavailability and lung targeting efficiency of azithromycin (AM) via two administration routes widely used in clinical practice, i.e., oral and intravenous routes, instead of transdermal route (by which the only marketed niosome-based drug delivery dermatologic products were given). The possible explanations for improved bioavailability and lung targeting efficacy were put forward here.

Results AMCNS-S (or AMCNS-L) had high bioavailability, for example, the oral (or intravenous) relative bioavailability of AMCNS-S (or AMCNS-L) to free AM increased to 273.19% (or 163.50%). After intravenous administration, AMCNS-S (or AMCNS-L) had obvious lung targeting efficiency, for example, the lung AM concentration of AMCNS-S (or AMCNS-L) increased 16 (or 28) times that of free AM at 12 h; the AM concentration of AMCNS-S (or AMCNS-L) in lung was higher than that in heart and kidney all the time.

Conclusions The development of niosome-based AM nanocarriers provides valuable tactics in antibacterial therapy and in non-lecithoid niosomal application.

Meng Zhong, Yue Feng, Hong Liao, Xueyuan Hu and Shengli Wan contributed equally to this work.

Electronic supplementary material The online version of this article (doi:10.1007/s11095-014-1382-7) contains supplementary material, which is available to authorized users.

M. Zhong • Y. Feng • H. Liao • X. Hu • S. Wan • M. Zhang • H. Xiong • Y. Zhou • J. Zhang (✉)
Medicine Engineering Research Center, Chongqing Medical University
Chongqing 400016, People's Republic of China
e-mail: zjqrae01@163.com

B. Zhu
West China School of Pharmacy, Sichuan University
Chengdu 610041, China

KEY WORDS administration route · azithromycin · bioavailability · cationic niosome · targeting efficiency

INTRODUCTION

Liposomal drug delivery systems, also called lecithoid nano/microparticles, have been going through from concept to clinical applications (1). Niosomes, being non-lecithoid nano/microparticles, were later occurred and somehow designed to overcome certain immanent shortcomings in liposomes which were mainly assigned to the phospholipid oxidation (2). Niosomes were biodegradable and biocompatible vesicular systems formed by non-ionic surfactants (3). Niosomes, having similar characteristics to liposomes, could carry both hydrophilic and lipophilic drugs. A number of niosome-based cosmetics produced by Lancôme for topical and transdermal deliveries of anti-ageing constituents are on the market (4). On the other hand, the evolution of niosomal drug delivery technology is still at the stage of infancy. As far as we know, there are only a very few niosome-based drug delivery dermatologic products used in clinic (5). However, niosomes do have shown promise in drug delivery, such as gene delivery (6), vaccine delivery (7), chemical drug delivery (8), and natural drug delivery (9). In case of antibiotics, niosome was investigated for topical delivery of gallidermin to highly accumulate in the skin (10), ophthalmic delivery of anti-conjunctivitis drug (such as chloramphenicol) to sustain release drug (11), parenteral delivery of antifungal drug (such as nystatin) to reduce its toxicity (12), oral delivery of anti-tuberculosis drug (such as rifampicin) to carry this drug together with other two synergic drugs (13).

Azithromycin (AM), a newly developed azalide antibiotic, has been widely used in the treatment of respiratory and gastrointestinal infections, such as pneumonia and gastroparesis (14–16). Recent *in vivo* studies indicated that the efficacy of AM was influenced by its concentration in the

target tissue of infection where pathogens were allowed to be exposed to (17). Unfortunately, the pharmacokinetic of free AM was characterized by very low serum concentrations and wide-spread tissue distribution in whole body (18). So the most common treatment was to administer orally with a high dose (500 mg per day) of AM in conventional tablets for 5 days or even longer (19). AM use was often associated with various adverse effects, such as diarrhoea, abdominal pain, and a recently discovered increased risk of death from cardiovascular causes (20,21). Developing novel suitable AM delivery systems with improved bioavailability and/or targeting efficiency had great clinical significance in reducing AM dosage, shortening the course of treatment, reducing adverse drug events, while increasing the clinical efficacy. However, the AM delivery systems developed in the past decade could not satisfy the clinical application requirements for desirable AM delivery systems, in fact, they were designed for other purposes: inhalation of liposomes for increasing permeable ability (22), inhalation of liquid aerosols for targeting to infected alveolar macrophages (23), oral delivery of cinnamon oil-based microemulsion to improve biocompatibility, ophthalmic delivery of *in situ* gel to prolong the duration of action (24), and rectal delivery of polyethylene glycol (PEG) suppository to facilitate pediatric use (25). Up to now, there has been still an urgent need to develop more suitable vesicles for effective and targeted delivery of AM via two administration routes widely used in clinical practice, i.e., oral or intravenous route. In addition, although there are currently no reports available for niosome-based AM delivery systems, they may be theoretically regarded as promising delivery systems for effective and targeted delivery of AM via oral or intravenous administration. Certainly encouraging experimental results are essential to support this practice hypothesis.

In this study, we fabricated cationic niosomes-based AM delivery systems (AMCNS) by applying similar formula but different preparation techniques. Here cationic niosomes (AMCNS-S and AMCNS-L stood for small-sized AMCNS and large-sized AMCNS, respectively) along with varied characteristics were designed to achieve high bioavailability and targeting efficiency of AM via oral and intravenous routes, instead of transdermal route (the only route of the marketed niosome-based drug delivery dermatologic products). AMCNS produced according to optimized formula was characterized by transmission electron micrograph (TEM), confocal laser scanning micrograph, and Fourier transformed infrared (FT-IR). The release behaviors of AMCNS in different release media (to mimic the gastrointestinal and circulating systemic environments, respectively) were evaluated by mathematical modeling and compared by the similarity factor (f_2) method recommended by United States Food and Drug Administration (U.S. FDA). The *in vivo* pharmacokinetic behavior, bioavailability, bioequivalence, distribution and targeting efficiency of AMCNS were investigated following oral and/or intravenous administration. The *in-vitro in-vivo* correlation of AMCNS defined by U.S. FDA was evaluated by mathematical modeling. The *in situ* absorption of AMCNS from gastrointestinal tract was further investigated by perfusion method to illustrate the possible reason of the increased oral bioavailability.

MATERIALS AND METHODS

Materials

Azithromycin (AM) was obtained from Shanghai Modern Pharmaceutical Co., Ltd. (Shanghai, China), purity >99%. Polysorbate 80 was purchased from Shenyu Pharmaceutical and Chemical Reagent Company Ltd. (Shanghai, China). Cholesterol was obtained from Tianma Fine Chemical Plant (Guangzhou, China). Octadecylamine was purchased from Shanghai Nanxiang Reagent Co., Ltd. (Shanghai, China). Methanol and acetonitrile of all HPLC grade were purchased from American TEDIA (TEDIA, USA). HPLC-grade water was purified by a Milli-Q system equipped with cellulose nitrate membrane filters (47 mm, 0.2 mm, Whatman, Maidstone, UK). All other reagents and solvents used in the study were of analytical grade. Animals, male Sprague Dawley rats (230±20 g) and Kunming strain mice (20±2 g), supplied by Laboratory Animal Center of Medical University (Chongqing, China) were acclimatized at a temperature of 25 ±3°C and a relative humidity of 70±5% under natural light/dark conditions for 1 week before dosing.

Preparation of AMCNS-S and AMCNS-L

The AMCNS-S was prepared by a thin-layer evaporation method (26), while the AMCNS-L was fabricated using the film-evaporation technology combined with freeze-thawing method (27,28). Briefly, 10 mL of chloroform solution containing 13 μmol of AM, 420 μmol of polysorbate 80, 1,300 μmol of cholesterol, 30 μmol of octadecylamine was prepared, followed by being removed under reduced pressure using a rotary evaporator (Yarong Biochemical Instrument Factory, Shanghai, China) at 40°C. (1) To make AMCNS-S, the resulting thin film was hydrated by adding 10 mL of pH 7.4 PBS and kept being evaporated at 45°C until the milky suspension (i.e., AMCNS-S) was obtained. (2) To make AMCNS-L, the resulting thin film was hydrated by adding 10 mL of pH 7.4 PBS containing 5% mannitol and kept being evaporated at 45°C until the milky suspension was obtained. Then the suspension was placed in freezer (at −20°C) overnight and thawed at 25°C. The suspension with 3 freeze-thaw cycles (i.e., AMCNS-L) was obtained.

In Vitro Characteristics of AMCNS

The morphological feature of AMCNS produced according to optimized formula was observed by the transmission electron microscopy (TEM H-7500, Hitachi, Japan) and a confocal laser microdissection system (Leica AS LMD, Wetzlar, Germany). The particle size of AMCNS-S was measured by a Zeta-Sizer (Nano-ZS 90, Malvern, Worcestershire, UK). The size of AMCNS-L was investigated using biomicroscopy (XSP-35-1600X, Phoenix, Shangrao, China). The zeta potential of AMCNS was measured by a Zeta-Sizer (Nano-ZS 90, Malvern, Worcestershire, UK). The characteristics of AM entrapped in the AMCNS were investigated using a FT-IR spectrophotometer (Spectrum One NTS, PerkinElmer Instruments Inc., Massachusetts, U.S.A.). The *in vitro* release of AM from AMCNS at 37°C was evaluated as follows: The AMCNS (5 mL) equivalent to 5 mg of AM was placed into dialysis tubes and immersed into 60 mL of different release media (pH 1.2 HCl solution, pH 6.8 phosphate buffered solution (PBS), and pH 7.4 PBS, respectively). The sink conditions were met. A milliliter of the release media was taken out and analyzed. The release behaviors of AMCNS were evaluated by mathematical modeling and compared by similarity factor (f_2) method (29).

Pharmacokinetic and Bioequivalence Evaluation of AMCNS

The animal experiments were approved by the Laboratory Animal Committee, Chongqing Medical University. Free AM, AMCNS-S and AMCNS-L were orally administered at the same AM dose of 200 mg/kg (or intravenously administered at the same AM dose of 100 mg/kg) to the Sprague–Dawley rats. The ophthalmic blood was collected at predetermined time points (5 min, 15 min, 30 min, 1 h, 2 h, 4 h, 6 h, 8 h, 12 h, 24 h and 48 h, respectively) and centrifuged at 3,000 rpm for 10 min. Each plasma sample was taken from the upper layer, and then 80 μL of sodium hydroxide and 2 mL of ether were added. The mixture was voxtexed for 5 min and then centrifuged at 3,000 r/min for 10 min. The ether layer was taken out and evaporated under nitrogen flow. The residue was reconstituted with 200 μL of methanol and centrifuged. An aliquot of supernatant (100 μL) was analyzed by HPLC. In brief, the stationary phase (Hypersil ODS-2 C18 column, 250 mm×4.6 mm, 5 μm, Elliot Corp. Dalian, China) was kept at 40°C. The mobile phase consisted of acetonitrile, isopropanol and 0.004 mol/L disodium hydrogen phosphates (60:15:25, v/v/v). The flow rate was 1.0 mL/min. The ultraviolet detector was set at 210 nm. The AM plasma concentration could be measured by HPLC, with good linearity in the range 1.0~50.0 μg/mL (r=0.9993, n=3). The average recoveries of high, middle, and low concentrations were 96.00, 98.67, and 99.36% respectively. Intra-and inter-day precisions expressed as the relative standard deviation for the method were 1.00~3.66% and 1.09~3.14%, respectively. It was suggested that the HPLC method was reliable for determination under the described conditions. The plasma AM concentration-time curves were drawn. The pharmacokinetic and bioequivalence evaluation were carried out using DAS 2.1.1 software (Mathematical Pharmacology Professional Committee of China, Shanghai, China). The *in-vitro in-vivo* correlation of AMCNS via oral administration was evaluated by comparing the calculated correlation coefficient of regression equations with the critical correlation coefficient (30,31). The equation was obtained by regressing the *in vivo* absorption fraction against the *in vitro* cumulative release rates. The *in vivo* absorption fractions were calculated using Loo-Riegelman method (for AMCNS-S) or Wagner-Nelson method (for AMCNS-L), respectively.

In Situ Gastrointestinal Absorption of AMCNS

The *in situ* gastrointestinal perfusion techniques were applied to investigate the AMCNS absorption in rats according to the previous reported method (32–34). For gastric absorption study, the stomachs of anesthetized rats were separately perfused with free AM, AMCNS-S or AMCNS-L which remained there for 2 h before they were drawn out and subjected to be analyzed by HPLC. In the intestinal absorption tests, each duodenal, jejunal, ileal and colonic segment (every enteric section was 10 cm long) was attached to the perfusion assembly consisting of a BT100-1L peristaltic pump (Baoding Longer Precision Pump Co. Ltd., Baoding, China) and equilibrated with Krebs-Ringer solution at a flow rate of 0.4 ml/min for a quarter of an hour. Intestinal segments were perfused with free AM, AMCNS-S or AMCNS-L at a flow rate of 0.2 ml/min for 1 h. One hour later, the remaining perfusion was analyzed by HPLC. The absorption parameters were calculated in accordance with formula 1 to 3. Formula 1: $K_a = (X_0 - X_t)/C_0\ t\pi r^2 l$; Formula 2: $PA\ (\%) = (X_0 - X_t)/X_0 \times 100\%$; Formula 3: $P_{eff} = R \times \ln(X_{in}/X_{out})/2\pi rl$. Where X_0 and X_t were the AM amount in perfusate at 0 h and t h, C_0 and C_t were the AM concentration in perfusate at 0 h and t h, X_{in} and X_{out} were the AM amounts in inlet and outlet perfusate, R was the perfusion flow rate, t was the perfusion time, r and l were the radius and length of the perfused intestinal segment.

Biodistribution and Lung Targeting of AMCNS

Free AM, AMCNS-S and AMCNS-L were intravenously administered to the Kunming mice at the same AM dose of 100 mg/kg. At predetermined time points (0.5, 3 and 24 h), the mice were sacrificed (the mice was sacrificed by cervical dislocation after femoral arterial blood sampling); their liver, spleen, heart, lung, and kidney were separately harvested and homogenized with physiological saline to obtain 25% homogenate. After that, the AM concentrations in these tissues were determined by a HPLC method described above. The lung targeting of AMCNS was analyzed by comparing the AM concentration in lung with that in other tissues.

Statistical Analysis

All data are shown as mean ± standard deviation unless particularly outlined. The Student's paired *t*-test was used to calculate statistical difference. A statistical significance was established at $P<0.05$. Pharmacokinetic and bioequivalence analyses were conducted using DAS software (Mathematical Pharmacology Professional Committee of China, Shanghai, China).

RESULTS

Principal Characteristics of AMCNS *In Vitro*

Both AMCNS-S and AMCNS-L were manufactured with high incorporation efficacy (80.46±0.54% and 92.87±0.77%, $n=3$, respectively). As shown in Fig. 1a and b, all the AMCNS (AMCNS referred to both AMCNS-S and AMCNS-L in all the following tests unless mentioned particularly) fabricated according to optimization formula (see the Supplementary Figure 1) were evenly dispersed in pH 7.4 phosphate buffer solution (PBS). They looked round and their structures kept almost intact without obvious aggregation. The spherical AMCNS-S with (0.95±0.10) μm had much smaller size than AMCNS-L with (5.87±1.80) μm in diameter; although they had similar zeta potential values (14.63±0.02) mV for AMCNS-S and (12.51±0.02) mV for AMCNS-L. The polydispersity index of AMCNS-S was (0.23±0.060). No obvious changes were observed when the AMCNS vesicles were placed at 4°C for 15 days (Supplementary Table 1). As shown in Fig. 1c, the characteristic peaks of AMCNS in the FT-IR spectrum were different from that of physical mixture. For example, the peaks of 2,920, 1,467 and 1,738 cm^{-1} in the FT-IR spectrum of AMCNS were obviously stronger than that in mixture. Moreover, the peaks of AM in FT-IR spectrum, such as 1,721 and 3,490 cm^{-1}, red shifted to 1,738 cm^{-1} or blue shifted to 3414 in the AMCNS spectrum, respectively. Above changes in FR-IR spectra suggested that AM had been entrapped into the niosomes (AMCNS). As shown in Fig. 1d, the entrapment of AM in the AMCNS systems could obviously slow down the *in vitro* release rates of AM in different release media (pH 1.2 HCl solution, pH 6.8 PBS, and pH 7.4 PBS, respectively) recommended by many national pharmacopoeias. Weibull models and first-order kinetic models could fit the release profiles of AMCNS and free AZM, respectively, regardless of the release medium type (Supplementary Table 2). Furthermore, a statistically significant difference was found between every pair of release profiles for AMCNS and free AM using the similar factor method (Supplementary Table 3) (35). Compared with AM, the AMCNS-L had sustained release effects.

Oral Delivery of AMCNS to Improve Pharmacokinetics and Bioavailability

The Sprague–Dawley rats were orally given with AMCNS and free AM at the same dose (200 mg/kg of AM). High performance liquid chromatography (HPLC) was used to determine the AM plasma concentration. As shown in Fig. 2a, the pharmacokinetic behavior of AMCNS-S was the most desirable compared to free AM and AMCNS-L. AM concentrations of AMCNS-S were much higher than that of free AM and AMCNS-L at almost every corresponding time points. After the experimental rats were given with free AM, AMCNS-S and AMCNS-L, the maximum AM plasma concentration appeared at 1.67, 6 and 3.33 h, respectively. The comparison of the main pharmacokinetic parameters of AMCNS-S, AMCNS-L and free AM was presented in Fig. 3. The *AUC*, *MRT*, C_{max}, T_{max}, *Cl* and K_a values of AMCNS-S (or AMCNS-L) were 2.73 (or 1.18) times, 1.76 (or 1.12) times, 1.78 (or 0.89) times, 3.60 (or 2) times, 0.44 (or 0.68) times, 0.18 (or 0.58) times that of free AM, respectively. By comparing the *AUC* values, the relative bioavailability (*RBA*) of AMCNS-S to free AM was calculated to be 273.19%, while the *RBA* of AMCNS-L to free AM, 117.76%. As we know, bioequivalence of two formulations was acceptable only when their 90% confidence intervals of *AUC* and C_{max} were within the bioequivalence acceptable range of 0.80–1.25 limits and 0.70–1.43 limits, respectively, and their T_{max} values were not significantly different ($p>0.05$) when using the Wilcoxon rank sum test. As shown in Fig. 2a, every two AM formulations among AMCNS-S, AMCNS-L and free AM were not bioequivalence. AMCNS-S had the highest bioavailability, maximum concentration and longest peak time.

The *in-vitro in-vivo* correlation of AMCNS was established by mathematical modeling. Briefly, the regression equations were listed as follows:

$$\text{For AMCNS}-\text{S}: \quad F_a = 0.9819\Upsilon + 1.0829, \quad r_{(4,0.01)} = 0.9565 > r_{critical(4,0.01)} = 0.9172 \tag{1}$$

$$\text{For AMCNS}-\text{L}: \quad F_a = 2.9075\Upsilon - 0.6407, \quad r_{(3,0.01)} = 0.9819 > r_{critical(3,0.01)} = 0.9587 \tag{2}$$

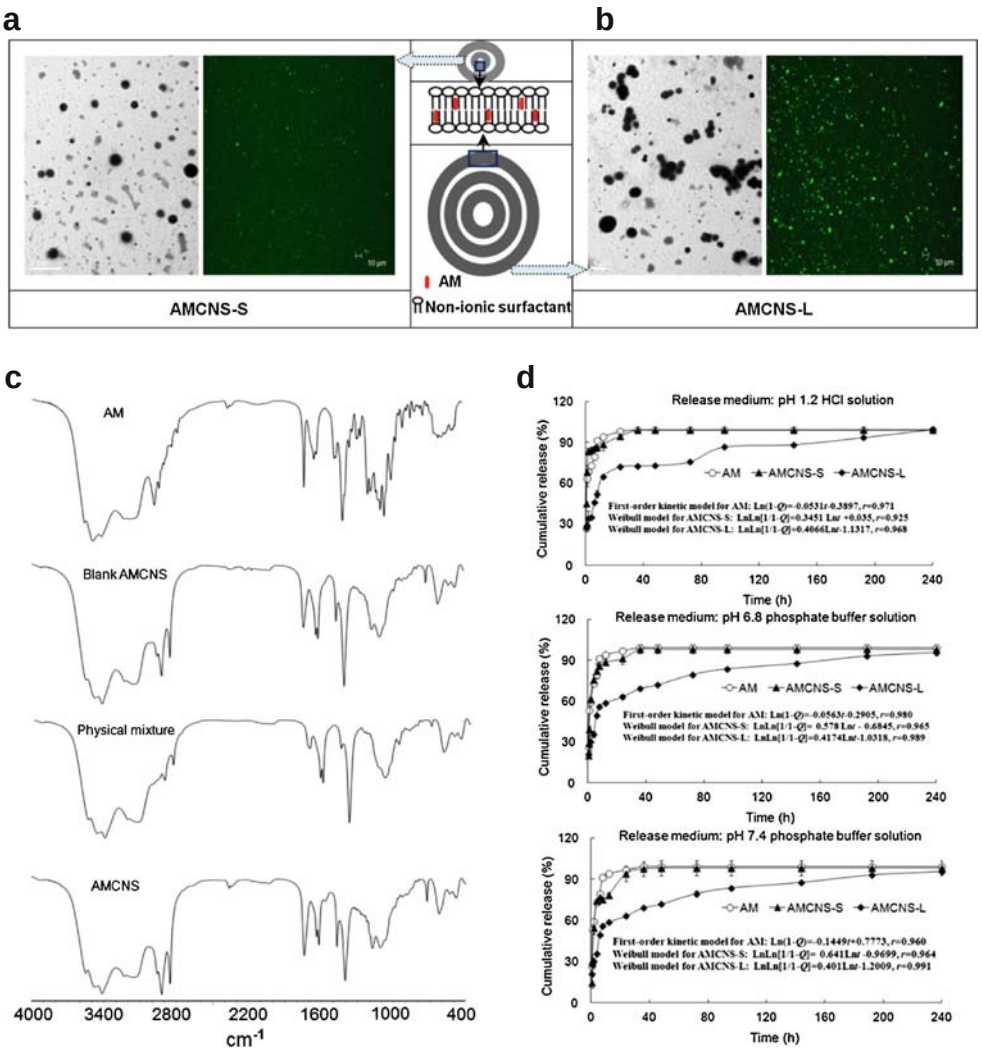

Fig. 1 *In vitro* characterization of AMCNS. (**a**) The photomicrographs of AMCNS-S, i.e., the transmission electron photomicrograph (left, bar, 2 μm) and the confocal laser scanning photomicrograph (right, bar, 10 μm), respectively. Schematic diagram of AMCNS-S (middle, the circle graph above). (**b**) Transmission electron photomicrograph (left, bar, 5 μm) and confocal laser scanning photomicrograph (right, bar, 10 μm) of AMCNS-L. Schematic diagram of AMCNS-L (middle, the circle graph below). (**c**) FT-IR spectra of AMCNS. (**d**) Release profiles of AM, AMCNS-S and AMCNS-L in different release media (the pH 1.2 HCl solution, pH 6.8 PBS and pH 7.4 PBS). $n = 3$. The data are shown as mean ± SD.

where F_a was the *in vivo* absorption fraction which calculated through Loo-Riegelman method (for AMCNS-S) or Wagner-Nelson method (for AMCNS-L) (30–32), Y was the *in vitro* cumulative release rate at pH 6.8 release medium, $r_{(n-2,\ 0.01)}$ was the correlation coefficient, n was the degree of freedom, here the n values were 6 (for AMCNS-S) and 5 (for AMCNS-L), respectively, 0.01 was the credibility level. $r_{critical\ (n-2,\ 0.01)}$ was the critical correlation coefficient. Obviously, there were *in-vitro in-vivo* correlations for both AMCNS-S and AMCNS-L.

Intravenous Delivery of AMCNS to Improve Pharmacokinetics and Bioavailability

After the experimental rats were intravenously given with AMCNS and free AM at the same dose (100 mg/kg of AM), their pharmacokinetic behaviors were presented in Fig. 2b. AM concentrations decreased sharply from the maximum values at 5 min (~40 μg/mL for all AM delivery systems) to lower levels at 8 h (<5 μg/mL for free AM, ~13 μg/mL for AMCNS-S and ~11 μg/mL for AMCNS-L, respectively). After that, AM concentrations decreased slowly to the very low levels (undetectable at 24 h for free AM, and at 48 h for AMCNS-S or AMCNS-L, respectively). The comparison of the main pharmacokinetic parameters of AMCNS-S, AMCNS-L and free AM was presented in Fig. 3. The *AUC*, *MRT*, and *Cl* of AMCNS-S (or AMCNS-L) were 1.92 (or 1.64) times, 1.92 (or 1.93) times, and 0.54 (or 0.64) times that of free AM, respectively. By comparing the *AUC* values, the relative bioavailability (*RBA*) of AMCNS-S to free AM was calculated to be 192.17%, while the *RBA* of AMCNS-L to free AM, 163.50%. As shown in Fig. 2b, neither AMCNS-S nor AMCNS-L was bioequivalent to free AM, while AMCNS-S and AMCNS-L were bioequivalent. Furthermore, AMCNS-S had the highest bioavailability, longest circulation time and lowest clearance rate.

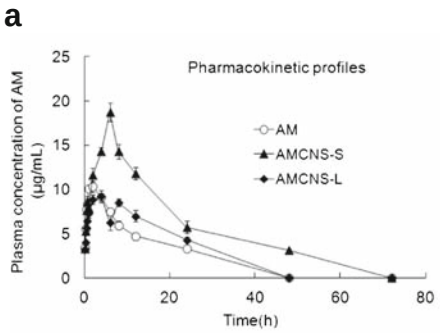

Bioequivalence comparison

Formulation 1 and 2	Parameter	90% confidential interval calculated	Bioequivalence standard	P value calculated	Bioequivalence
AMCNS-S and AM	AUC	41-45%	80-125%	-	No
	C_{max}	54-58%	70-143%	-	No
	T_{max}	-	-	<0.05	No
AMCNS-L and AM	AUC	77-89%	80-125%	-	No
	C_{max}	105-120%	70-143%	-	Yes
	T_{max}	-	-	>0.05	Yes
AMCNS-S and AMCNS-L	AUC	186-200%	80-125%	-	No
	C_{max}	187-212%	70-143%	-	No
	T_{max}	-	-	<0.05	No

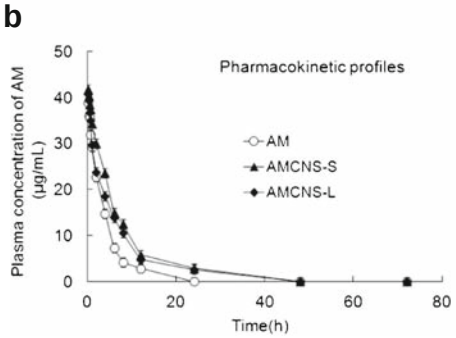

Bioequivalence comparison

Formulation 1 and 2	Parameter	90% confidential interval calculated	Bioequivalence standard	P value calculated	Bioequivalence
AMCNS-S and AM	AUC	45-60%	80-125%	-	No
	C_{max}	82-104%	70-143%	-	Yes
	T_{max}	-	-	>0.05	Yes
AMCNS-L and AM	AUC	51-71%	80-125%	-	No
	C_{max}	83-107%	70-143%	-	Yes
	T_{max}	-	-	>0.05	Yes
AMCNS-S and AMCNS-L	AUC	115-118%	80-125%	-	Yes
	C_{max}	100-105%	70-143%	-	Yes
	T_{max}	-	-	>0.05	Yes

Fig. 2 *In vivo* pharmacokinetic profiles (i.e., plasma concentration-time curves) and the bioequivalence evaluation of AMCNS and free AM after (**a**) oral administration at the same AM dose of 200 mg/kg and (**b**) intravenous administration at the same dose AM of 100 mg/kg, respectively. Six rats per group. The data are shown as mean ± SD.

Perfusion of AMCNS to Improve the *In Situ* Gastrointestinal Absorption

AMCNS-S was superior to AMCNS-L in enhancement of gastrointestinal (GI) absorption of AM. Comparison among AMCNS and free AM in different gastrointestinal segments of gastrointestinal absorption rate constant (K_a) and absorption percentage (*PA*), and intestinal effective permeability (P_{eff}) were presented in Fig. 4a and b.

A small amount of free AM (~10%) could be absorbed from the stomach. The *PA* values of AMCNS-S and AMCNS-L increased to ~27 and ~18% respectively. The intestine was the major site for AM absorption. AMCNS-S had the highest K_a (or P_{eff}) values while free AM had the least

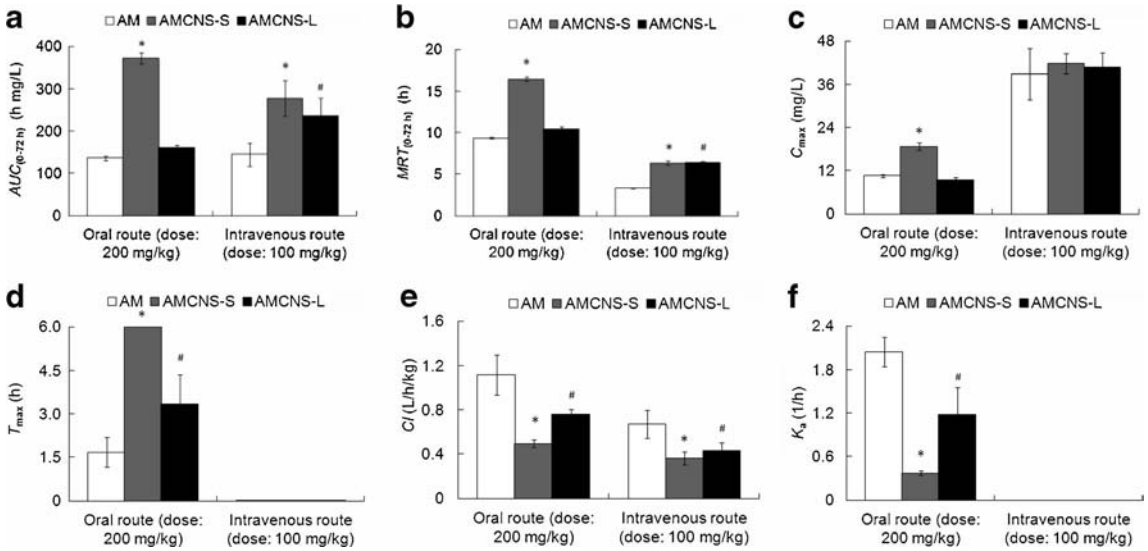

Fig. 3 The comparison of the main pharmacokinetic parameters of AMCNS and free AM via oral (at the identical dose of 200 mg/kg of AM) and intravenous (at the dose of 100 mg/kg of AM) routs, respectively, Six rats per group. The data are shown as mean ± SD. $^{*}P < 0.05$ and $^{\#}P < 0.05$ indicate significant differences between AMCNS-S (or AMCNS-L) and free AM. (**a**) The *AUC* (area under the plasma concentration-time curve) values of AMCNS and free AM in 72 h. (**b**) The *MRT* (mean residence time) values of AMCNS and free AM in 72 h. (**c**) The C_{max} (maximum concentration) values of AMCNS and free AM. (**d**) The T_{max} (peak time) values of AMCNS and free AM. (**e**) The *Cl* (clearance rate) values of AMCNS and free AM. (**f**) The k_a (absorption rate constant) values of AMCNS and free AM.

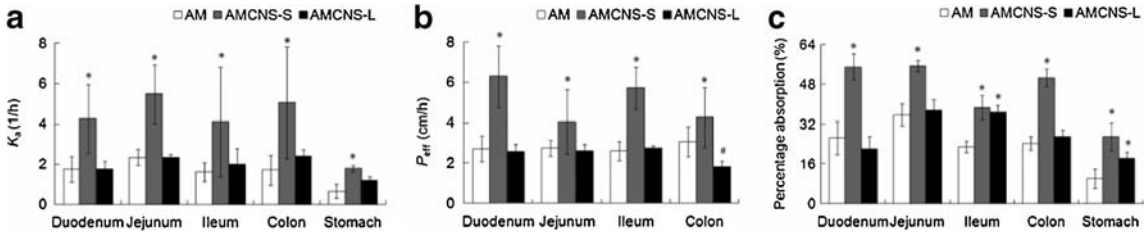

Fig. 4 The absorption rate constant (K_a), effective permeability (P_{eff}) and percent absorption of AMCNS and free AM through stomach absorption and single pass intestinal perfusion studies. Six rats per group. The data are shown as mean ± SD. $^{*}P < 0.05$ and $^{\#}P < 0.05$ indicate significant differences between the group of AMCNS-S (or AMCNS-L) and the group of free AM.

values among AMCNS-S, AMCNS-L and free AM in every corresponding intestinal segment. The K_a (or P_{eff}) values of AMCNS-S in the duodenum, jejunum, ileum, and colon were 2.41 (or 2.34), 2.35 (or 1.47), 2.54 (or 2.20), and 2.95 (or 1.40) times that of free AM, respectively. The study on intestinal absorption of AMCNS-S in different regions of rat intestine indicated that (1) the absorption percentages in the duodenum, jejunum and colon were almost the same high, and they were much higher than that in the ileum. (2) The permeabilities in the duodenum and ileum were almost the same high, and they were much higher than that in the jejunum and colon. Compared with AMCNS-S, AMCNS-L altered the absorption rate and permeability of AM in intestinal tract to a lesser extent. It was worthy of notice that AMCNS-L obviously increased the absorption percent in ileum (1.60-folds that of free AM) which might be partly due to the increased absorption rate constant.

Intravenous Delivery of AMCNS to Improve Lung Targeting

When AMCNS and free AM were intravenously administered to Kunming mice, the AM concentrations in different tissues (liver, spleen, heart, lung and kidney) at predetermined time points were determined and compared (Fig. 5). For free AM, the lung AM concentration was ~17 μg/mL at 0.5 h, and decreased to ~13 μg/mL at 3 h and ~0.5 μg/mL at 12 h, respectively. Beside the AM concentration in lung, the AM concentrations in other four tissues, i.e., spleen, liver, heart and kidney, were quite low (<1 μg/mL) at 12 h. In addition, the AM concentrations in spleen and liver were higher than that in lung all the time. Moreover, the AM concentrations in heart was higher than that in lung at 0.5 and 12 h, and a little lower than that in lung at 3 h. Both AMCNS-L and AMCNS-S changed the pulmonary AM distribution *in vivo*. Briefly, for AMCNS-L, (1) the lung AM concentration was ~20 μg/mL at 0.5 h, and increased to ~34 μg/mL at 3 h followed by decreasing to ~14 μg/mL at 12 h, respectively. (2) Especially, the lung AM concentration for AMCNS-L at 12 h remained high and it was even higher than that for free AM at 3 h. (3) At 0.5 h, the AM concentration in lung was almost the same high as that in spleen, higher than that in liver, heart and kidney. At 3 and 12 h, the AM concentration in lung was much higher than that in other tissues. While for AMCNS-S, (1) compared with AMCNS-L and free AM, the lung AM concentration was the highest (~25 μg/mL) at 0.5 h. However, at 3 and 12 h, the lung AM concentrations (~17 μg/mL at 3 h and ~8 μg/mL at 12 h) were much higher than that of free AM and lower than that of AMCNS-L, respectively. (2) Similar to free AM, the AM concentrations in spleen and liver were higher than that in lung all the time. However, the AM concentrations in heart and kidney were lower than that in lung all the time.

DISCUSSIONS

Being a non-lecithoid nanocarrier, niosome had its own intrinsic advantages over liposome (such as better stability by avoiding phospholipid oxidation) (2). Niosomes had shown great potential in delivery of biomolecules (such as siRNA and vaccine), chemical and natural drug (3,36). However, on the market there were only a very few niosome products (all of they are used for treatment of dermatology) (5). On the other hand, although identifying novel antibiotics remained a priority, the development of suitable delivery systems for currently used antibiotics might represent a cost-effective and

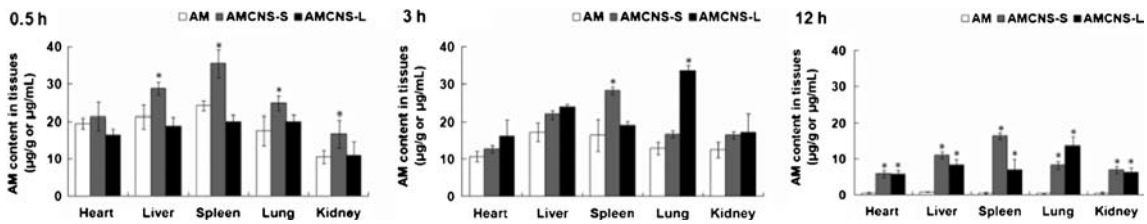

Fig. 5 *In vivo* distribution of intravenously administered AMCNS and free AM in Kunming mice at 0.5, 3, and 12 h, respectively. Six mice per group. The data are shown as mean ± SD. $^{*}P < 0.05$ indicate significant differences between the group of AMCNS-S (or AMCNS-L) and the group of free AM.

promising alternative. As mentioned before, there has been unmet clinical need to develop suitable vesicles for effective and lung targeted delivery of AM via two most common administration routes (i.e., oral or intravenous route). So, in this study, AM was chosen as model drug, and the potential of cationic niosomes to smartly deliver AM, as well as to improve bioavailability and lung targeting efficiency, was investigated. Currently, there are no reports available for niosome-based AM delivery systems.

After oral administration, both AMCNS-S and AMCNS-L improved pharmacokinetic behavior and bioavailability of free AM, albeit to different extents. Compared to free AM, the *AUC* and *MRT* values of AMCNS-S (or AMCNS-L) increased by 2.73 (or 1.18) folds and 1.76 (1.12) folds, while *Cl* value decreased as 0.44 (or 0.68) folds; AMCNS-S (or AMCNS-L) given orally had larger *AUC*, longer *MRT* and slower *Cl* values, which might provide beneficial therapeutic effects of long-acting AM. Furthermore, in our study, the bioavailability of free AM in rat administered orally relative to intravenously was ~47%, which was comparable to the value of 38% for oral AM product in humans reported by Kauss *et al.* (25). The relative bioavailability of AMCNS-S (or AMCNS-L, given orally) to free AM (given orally) was 273.19% (or 117.76%); the absolute bioavailability of AMCNS-S (or AMCNS-L, given orally) to free AM (given intravenously) was 128.64% (or 55.45%). Bioavailability was a term used to describe the degree to which a drug became available to exert a pharmacologic effect into the bloodstream after administration. The fact that AMCNS-S given orally had very higher absolute bioavailability (128.64%>100%) suggested that: (1) AMCNS-S given orally exerted a better pharmacologic effect compared with free AM even given intravenously. (2) To achieve similar pharmacologic effect to that of free AM given intravenously, the dose of AMCNS-S could be reduced, and then the unfavorable side effects or the treatment duration might be reduced. (3) To achieve similar pharmacologic effect to that of free AM given orally, the dose of AMCNS-S could be markedly reduced, and then the unfavorable side effects or the treatment duration might be greatly reduced. (4) Similar statements could be made about the data for AMCNS-L given orally.

In addition, for oral drugs, bioavailability reflected the rate and extent of GI tract absorption. Our further *in situ* absorption study indicated that the markedly improved oral bioavailability of AMCNS-S (or AMCNS-L) was likely due to the increased GI absorption especially the intestinal absorption. Compared to free AM, the absorption rates (or permeabilities) of AMCNS-S in the duodenum, jejunum, ileum, and colon increased by 2.41 (or 2.34) folds, 2.35 (or 1.47) folds, 2.54 (or 2.20) folds, and 2.95 (or 1.40) folds, respectively. It was impressive that AMCNS-S increased the absorption in every intestinal segment. In comparison with AMCNS-S, AMCNS-L only obviously increased the absorption percent in ileum (1.60-folds that of free AM), mostly due to the increased absorption rate constant. The possible reasons for improved absorption of AMCNS-S were listed as follows: (1) solubilization of AM by encapsulating into the cationic niosomes with different sizes; (2) high dispersibility of AM in cationic niosomes; (3) protection from enzymatic oxidation (AM was the substrate of CYP3A enzyme) (37); (4) prevention from P-gp mediated AM efflux (water insoluble AM was a P-gp substrate) by embedding AM into the niosomal system containing constituents such as the surfactants which could act as P-gp inhibitors; (5) the sustained release of AM from AMCNS; (6) lymphatic transport of niosomes by crossing the anatomical barrier of gastrointestinal tract via transcytosis of M cells of Peyer's patches in the intestinal lymphatic tissues (38). The reason for the notable absorption improvement of AMCNS-L only in ileum was unclear.

Similar analysis could be carried out about the data for AMCNS-S and AMCNS-L given intravenously. After intravenous administration, compared to free AM, the *AUC* and *MRT* values of AMCNS-S (or AMCNS-L) increased by 1.92 (or 1.64) folds and 1.92 (1.93) folds, while *Cl* value decreased as 0.54 (or 0.64) folds; AMCNS-S (or AMCNS-L) having longer circulation time and lower clearance rates values, might also provide beneficial therapeutic effects of long-acting AM. The greatly improved bioavailabilities of AMCNS-S (192.17%) and AMCNS-L (163.50%) after intravenous administration were likely due to the sustained AM release. The *in vivo* sustained AM release of AMCNS-S (or AMCNS-L) in blood was in agreement with the *in vitro* release of AMCNS-S (or AMCNS-L) in pH 7.4 PBS medium. Compared to free AM, AMCNS-S and AMCNS-L with higher bioavailability clearly indicated higher therapy efficacy, shorter treatment duration, as well as lower undesirable adverse effects.

When AMCNS-L and AMCNS-S were intravenously administered to mice, both of them altered the tissue AM distribution, chiefly improved the lung targeting efficacy. Take AMCNS-L for example, one hand, its lung concentration was much higher than that of free AM (such as ~34 μg/mL *versus* ~13 μg/mL at 3 h); on the other hand, its lung concentration was much higher than AM concentration in other tissues. Since AM was potent against a number of intracellular parasitic pathogens which survived or intracellularly multiplied in alveolar macrophages (17), high lung targeting efficacy was beneficial to the effective treatments for respiratory diseases, simultaneously to decrease the side effects produced by high concentrations in other normal tissue (such as decreasing the risk of death from cardiovascular causes). AMCNS-L was mainly prepared for injectable passive lung targeting. The possible explanations for lung targeting efficacy were listed as follows: (1) the "mechanical trapping" effect of the pulmonary capillary network. Previous studies showed that carriers ranged from 3 to 30 μm exhibited significant lung targeting

characteristics (39–41). (2) Positive charge of carrier was beneficial for drug to become pooled in the lung. Previous studies showed that systemic delivery of cationic vectors mediates efficient retention within the lung, mainly as a result of interaction of the vectors with serum proteins (42–44). (3) The "adhesive trapping" effect of the pulmonary capillary proteins. Adhesive proteins might act as a kind of glue to trap cells, although the exact physical basis of this trapping was still not clear (http://www.phy.ohiou.edu/~tees/current_research.html). (4) Compared to free AM, AMCNS had longer blood circulation time which was beneficial for AM able to achieve the targeted lung. AMCNS-L had much higher targeting efficacy than AMCNS-S at 3 h, higher at 12 h. However, it should be noted that AMCNS-S had a higher targeting efficacy than AMCNS-L at 0.5 h and the reason was still unclear. Besides injectable administration, carriers were reported to achieve lung targeting via other routes, such as inhalable (45) and intranasal administration but no oral administration (46). In our study, when free AM, AMCNS-S or AMCNS-L was orally given to mice at the dose of 200 mg/kg AM, the AM concentrations in lung tissues were undetectable under experimental conditions (data not shown).

Additionally, our study showed that both AMCNS-S and AMCNS-L encapsulated AM well which was evidenced by high incorporation efficacies (~80 and ~93%, respectively). The entrapment efficiencies of AMCNS were to a comparable degree with niosomes containing other lipophilic drugs, such as griseofulvin niosome, zidovudine niosome and hydroxycamptothecin niosome (their incorporation efficacies were ~77, ~80 and ~93%, respectively) (38,47,48). Furthermore, compared to free AM, AMCNS especially AMCNS-L, had obvious *in vitro* sustained release characteristics in release media of pH 1.2 HCl solutions, pH 6.8 PBS, and pH 7.4 PBS which simulated gastric juice, intestinal fluid and blood (or tissue) fluid, respectively; AMCNS especially AMCNS-S, had distinct *in vivo* absorptive characteristics via oral administration. It was found that there were *in-vitro in-vivo* correlations for both AMCNS-S and AMCNS-L by using a mathematical modeling method. Since *in-vitro in-vivo* correlation had been defined by U.S. FDA as "a predictive mathematical model describing the relationship between an *in-vitro* property of a dosage form and an *in-vivo* response", the good *In-vitro in-vivo* correlation of AMCNS suggested that the *in vitro* release data might predict the *in vivo* situation to a certain extent.

CONCLUSION

The development of cationic niosomes-based AM nanocarriers with different sizes to improve bioavailability and lung targeting efficiency provides valuable tactics in antibacterial therapy and in non-lecithoid niosomal application. In this study, we fabricated AMCNS-S and AMCNS-L by applying similar formulas but different preparation techniques. The *in vivo* biological properties of AMCNS-S and AMCNS-L were investigated via oral and intravenous administration routes (the widely used routes in clinically practice) instead of transdermal route (the only route of the marketed niosome-based drug delivery dermatologic products). The oral bioavailability of AMCNS-S (or AMCNS-L) to free AM increased to 273.19% (or 117.76%), while its intravenous relative bioavailability increased to 192.17% (or 163.50%). The markedly improved oral bioavailability of AMCNS-S (or AMCNS-L) was likely due to the increased GI absorption especially the intestinal absorption. The possible reasons for improved absorption of AMCNS-S were mainly ascribed to solubilization, high dispersibility and sustained release of AM, protection from enzymatic oxidation and P-gp mediated EDA efflux, and lymphatic transport. But the reason for the notable absorption improvement of AMCNS-L only in ileum was unclear. The greatly improved bioavailabilities of AMCNS-S and AMCNS-L after intravenous administration were likely due to the sustained AM release. After intravenous administration, AMCNS-S (or AMCNS-L) had obvious lung targeting efficiency, for example, the lung AM concentration of AMCNS-S (or AMCNS-L) increased 16 (or 28) times that of free AM at 12 h; the AM concentration of AMCNS-S (or AMCNS-L) in lung was higher than that in heart and kidney all the time. The possible explanations for lung targeting efficacy of AMCNS were mainly ascribed to mechanical and adhesive trapping effects of the pulmonary capillary network, positive charge of carrier and long blood circulation time. In all, AMCNS-S and AMCNS-L with different sizes had different built-in features, so they may be promising carriers for smart delivery of AM via oral or intravenous administration to meet different clinical application requirements.

ACKNOWLEDGMENTS AND DISCLOSURES

This research was partially supported by grants from Chongqing Natural Science Foundation (CSCT2012JJB10027), and Chongqing Education Committee Fund (the excellent university personnel financial aid plan, KJ120321).

REFERENCES

1. Allen TM, Cullis PR. Liposomal drug delivery systems: from concept to clinical applications. Adv Drug Deliv Rev. 2013;65(1):36–48.
2. Mahale NB, Thakkar PD, Mali RG, Walunj DR, Chaudhari SR. Niosomes: novel sustained release nonionic stable vesicular systems–an overview. Adv Colloid Interf Sci. 2012;183–184:46–54.
3. Rajera R, Nagpal K, Singh SK, Mishra DN. Niosomes: a controlled and novel drug delivery system. Biol Pharm Bull. 2011;34(7):945–53.

4. Puglia C, Bonina F. Lipid nanoparticles as novel delivery systems for cosmetics and dermal pharmaceuticals. Expert Opin Drug Deliv. 2012;9(4):429–41.
5. Hamishehkar H, Rahimpour Y, Kouhsoltani M. Niosomes as a propitious carrier for topical drug delivery. Expert Opin Drug Deliv. 2013;10(2):261–72.
6. Manosroi J, Khositsuntiwong N, Manosroi W, Götz F, Werner RG, Manosroi A. Potent enhancement of transdermal absorption and stability of human tyrosinase plasmid (pAH7/Tyr) by Tat peptide and an entrapment in elastic cationic niosomes. Drug Deliv. 2013;20(1):10–8.
7. Vyas SP, Singh RP, Jain S, Mishra V, Mahor S, Singh P, *et al.* Non-ionic surfactant based vesicles (niosomes) for non-invasive topical genetic immunization against hepatitis B. Int J Pharm. 2005;296(1–2):80–6.
8. Tavano L, Muzzalupo R, Mauro L, Pellegrino M, Andò S, Picci N. Transferrin-conjugated Pluronic niosomes as a new drug delivery system for anticancer therapy. Langmuir. 2013. doi:10.1021/la4021383.
9. Mandal S, Banerjee C, Ghosh S, Kuchlyan J, Sarkar N. Modulation of the photophysical properties of curcumin in nonionic surfactant (Tween-20) forming micelles and niosomes: a comparative study of different microenvironments. J Phys Chem B. 2013;117(23):6957–68.
10. Manosroi A, Khanrin P, Lohcharoenkal W, Werner RG, Götz F, Manosroi W, *et al.* Transdermal absorption enhancement through rat skin of gallidermin loaded in niosomes. Int J Pharm. 2010;392(1–2):304–10.
11. Yasin MN, Hussain S, Malik F, Hameed A, Sultan T, Qureshi F, *et al.* Preparation and characterization of chloramphenicol niosomes and comparison with chloramphenicol eye drops (0.5%w/v) in experimental conjunctivitis in albino rabbits. Pak J Pharm Sci. 2012;25(1):117–21.
12. El-Ridy MS, Abdelbary A, Essam T, El-Salam RM, Kassem AA. Niosomes as a potential drug delivery system for increasing the efficacy and safety of nystatin. Drug Dev Ind Pharm. 2011;37(12):1491–508.
13. Mehta SK, Jindal N. Formulation of tyloxapol niosomes for encapsulation, stabilization and dissolution of anti-tubercular drugs. Colloids Surf B: Biointerfaces. 2013;101:434–41.
14. Berger A, Edelsberg J, Oster G, Huang X, Weber DJ. Patterns of initial antibiotic therapy for community-acquired pneumonia in U.S. hospitals, 2000 to 2009. Am J Med Sci. 2013. doi:10.1097/MAJ.0b013e318294833f.
15. Nirmala MJ, Mukherjee A, Chandrasekaran N. Design and formulation technique of a novel drug delivery system for azithromycin and its anti-bacterial activity against staphylococcus aureus. AAPS PharmSciTech. 2013;14(3):1045–54.
16. Potter TG, Snider KR. Azithromycin for the treatment of gastroparesis. Ann Pharmacother. 2013;47(3):411–5.
17. Togami K, Chono S, Morimoto K. Subcellular distribution of azithromycin and clarithromycin in rat alveolar macrophages (NR8383) in vitro. Biol Pharm Bull. 2013;36(9):1494–9.
18. Magis-Escurra C, Alffenaar JW, Hoefnagels I, Dekhuijzen PN, Boeree MJ, van Ingen J, *et al.* Pharmacokinetic studies in patients with nontuberculous mycobacterial lung infections. Int J Antimicrob Agents. 2013;42(3):256–61.
19. Harding-Esch EM, Sillah A, Edwards T, Burr SE, Hart JD, Joof H, *et al.* Mass treatment with azithromycin for trachoma: when is one round enough? Results from the PRET Trial in the Gambia. PLoS Negl Trop Dis. 2013;7(6):e2115.
20. de Diego A, Milara J, Martinez E, Palop M, León M, Cortijo J. Effects of long-term azithromycin therapy on airway oxidative stress markers in non-cystic fibrosis bronchiectasis. Respirology. 2013. doi:10.1111/resp.12130.
21. Svanström H, Pasternak B, Hviid A. Use of azithromycin and death from cardiovascular causes. N Engl J Med. 2013;368(18):1704–12.
22. Wallace SJ, Nation RL, Li J, Boyd BJ. Physicochemical aspects of the coformulation of colistin and azithromycin using liposomes for combination antibiotic therapies. J Pharm Sci. 2013;102(5):1578–87.
23. Togami K, Chono S, Morimoto K. Aerosol-based efficient delivery of azithromycin to alveolar macrophages for treatment of respiratory infections. Pharm Dev Technol. 2013;18(6):1361–5.
24. Vijaya C, Goud KS. Ion-activated in situ gelling ophthalmic delivery systems of azithromycin. Indian J Pharm Sci. 2011;73(6):615–20.
25. Kauss T, Gaubert A, Boyer C, Ba BB, Manse M, Massip S, *et al.* Pharmaceutical development and optimization of azithromycin suppository for paediatric use. Int J Pharm. 2013;441(1–2):218–26.
26. Bangham AD, Standish MM, Watkins JC. Diffusion of univalent ions across the lamellae of swollen phospholipids. J Mol Biol. 1965;13(1):238–52.
27. Ozaki K, Hayashi M. Cryoprotective effects of cycloinulohexaose on freezing and freeze-drying of liposomes. Chem Pharm Bull. 1996;44(11):2116–20.
28. Anchordoquy TJ, Girouard LG, Carpenter JF, Kroll DJ. Stability of lipid/DNA complexes during agitation and freeze-thawing. J Pharm Sci. 1998;87(9):1046–51.
29. Tan Q, Li Y, Wu J, Mei H, Zhao C, Zhang J. An optimized molecular inclusion complex of diferuloylmethane: enhanced physical properties and biological activity. Int J Nanomedicine. 2012;7:5285–393.
30. Honório Tda S, Pinto EC, Rocha HV, Esteves VS, Dos Santos TC, Castro HC, *et al.* In vitro-in vivo correlation of Efavirenz Tablets Using GastroPlus®. AAPS PharmSciTech. 2013;14(3):1244–54.
31. Park JS, Shim JY, Park JS, Lee MJ, Kang JM, Lee SH, *et al.* Formulation variation and in vitro-in vivo correlation for a rapidly swellable three-layered tablet of tamsulosin HCl. Chem Pharm Bull. 2011;59(5):529–35.
32. Perioli L, Mutascio P, Pagano C. Influence of the nanocomposite MgAl-HTlc on gastric absorption of drugs: in vitro and ex vivo studies. Pharm Res. 2013;30:156–66.
33. Samiei N, Mangas-Sanjuan V, González-Álvarez I, Foroutan M, Shafaati A, Zarghi A, *et al.* Ion-pair strategy for enabling amifostine oral absorption: rat in situ and in vivo experiments. Eur J Pharm Sci. 2013;49:499–504.
34. Tan QY, Hu NN, Liu GD, Yin HF, Zhang L, Wang H, *et al.* Role of a novel pyridostigmine bromide-phospholipid nanocomplex in improving oral bioavailability. Arch Pharm Res. 2012;35:499–508.
35. Tan Q, Jiang R, Xu M, Liu G, Li S, Zhang J. Pyridostigmine bromide nanosized microcapsules for sustained release: process optimization and characteristics evaluation. Int J Nanomedicine. 2013;8:737–45.
36. Manosroi A, Chaikul P, Abe M, Manosroi W, Manosroi J. Melanogenesis of methyl myristate loaded niosomes in B16F10 melanoma cells. J Biomed Nanotechnol. 2013;9(4):626–38.
37. Ohno Y, Hisaka A, Suzuki H. General framework for the quantitative prediction of CYP3A4-mediated oral drug interactions based on the AUC increase by coadministration of standard drugs. Clin Pharmacokinet. 2007;46(8):681–96.
38. Jadon PS, Gajbhiye V, Jadon RS, Gajbhiye KR, Ganesh N. Enhanced oral bioavailability of griseofulvin via niosomes. AAPS PharmSciTech. 2009;10:1186–92.
39. Deshmukh M, Kutscher HL, Gao D, Sunil VR, Malaviya R, Vayas K, *et al.* Biodistribution and renal clearance of biocompatible lung targeted poly(ethylene glycol) (PEG) nanogel aggregates. J Control Release. 2012;164(1):65–73.
40. Lu B, Zhang J, Yang H. Non phospholipid vesicles of carboplatin for lung targeting. Drug Deliv. 2003;10(2):87–94.
41. Wei Y, Xue Z, Ye Y, Huang Y, Zhao L. Paclitaxel targeting to lungs by way of liposomes prepared by the effervescent dispersion technique. Arch Pharm Res. 2013. doi:10.1007/s12272-013-0181-8.
42. Jinturkar KA, Anish C, Kumar MK, Bagchi T, Panda AK, Misra AR. Liposomal formulations of etoposide and docetaxel for p53

mediated enhanced cytotoxicity in lung cancer cell lines. Biomaterials. 2012;33(8):2492–507.
43. Tamilvanan S, Khanum R, Senthilkumar SR, Muthuraman M, Rajasekharan T. Studies on ocular and parenteral application potentials of azithromycin- loaded anionic, cationic and neutral-charged emulsions. Curr Drug Deliv. 2013;10(5):572–86.
44. Tokatlian T, Segura T. siRNA applications in nanomedicine. Wiley Interdiscip Rev Nanomed Nanobiotechnol. 2010;2(3):305–15.
45. Chattopadhyay S. Aerosol generation using nanometer liposome suspensions for pulmonary drug delivery applications. J Liposome Res. 2013;23(4):255–67.
46. Koyama K, Nakai D, Takahashi M, Nakai N, Kobayashi N, Imai T, *et al.* Pharmacokinetic mechanism involved in the prolonged high retention of laninamivir in mouse respiratory tissues after intranasal administration of its prodrug laninamivir octanoate. Drug Metab Dispos. 2013;41(1):180–7.
47. Ruckmani K, Sankar V. Formulation and optimization of Zidovudine niosomes. AAPS PharmSciTech. 2010;11(3):1119–27.
48. Hong M, Zhu S, Jiang Y, Tang G, Pei Y. Efficient tumor targeting of hydroxycamptothecin loaded PEGylated niosomes modified with transferrin. J Control Release. 2009;133(2):96–102.